Final Report
for

A Demonstration of Multi-Variate Visualization and Optimization Methods for an Aircraft Energy System Application

By

Dr. Brian German
Principal Investigator

Assistant Professor
Associate Director, Aerospace Systems Design Laboratory (ASDL)
Daniel Guggenheim School of Aerospace Engineering
Georgia Institute of Technology
Atlanta, GA 30332-0150

February 3, 2011

Table of Contents

Executive Summary

This report describes a research project that was conducted at Georgia Tech under contract to Doty Consulting Services to demonstrate multi-variate design space exploration methods for an aircraft energy system of interest to the U.S. Air Force. An aircraft thermal architecture including a fuel thermal management system, an air cycle machine for ECS cooling, and a turbofan engine were modeled in MATLAB. The model employs First Law and Second Law thermodynamic analyses to determine energy transfers and entropy generation and is parameterized in terms of relevant system design variables including temperatures, heat exchanger properties, flow rates, and pressure ratios. The simulation is coded in an object-oriented framework that allows the flexibility to model a wide variety of thermal system architectures. This modeling tool will be provided as a deliverable of this project for use by Doty Consulting and AFRL.

Two parametric design space exploration studies were conducted for the baseline thermal system architecture using multi-variate data visualization and optimization approaches based on parallel coordinates. In the first study, heat transfer rates were specified directly, and in the second study, heat exchanger effectiveness was specified. The investigations focused on three primary aspects: (1) Identification of import design parameters driving system performance, (2) Second Law feasibility of heat transfers, and (3) optimality in terms of engine thrust and fuel burn performance. A design of experiments (DOE) was run using the MATLAB model in order to populate the design space for the studies. To allow rapid and interactive trade space explorations with parallel coordinates, artificial neural network surrogate models were regressed based on the DOE results.

The results of the studies indicate the significant utility of multi-variate visualization methods such as parallel coordinates for exploring the parametric design spaces of aircraft thermal systems to determine feasibility and optimality. The multi-variate graphical methods used in the project are an outgrowth of prior Georgia Tech work in the development of Rave, an interactive design data visualization tool. Rave has been released open source and is now available for download by Doty Consulting and AFRL researchers at www.rave.gatech.edu. The parallel coordinate functionality in Rave was substantially improved during this project by incorporation of new user interaction techniques and filtering methods.

Introduction

Aircraft thermal systems have become increasingly important for assuring operational capability of high performance aircraft. Modern military fighters and strike aircraft have high thermal loads associated with the propulsion system, actuators, avionics, and electronic payloads. These vehicles are also increasingly constructed of composite materials which decrease opportunities to reject heat through the aircraft skin, and they are often designed with stringent low observable requirements that limit the use of ambient air inlets for ram air cooling systems. These thermal issues pose extraordinary challenges in the design and optimization of thermal management systems.

Thermal management design is recognized as one aspect of a broader set of challenges associated with matching aircraft subsystems to the airframe design, performance, and operability requirements. Another challenge is the design of high power electrical systems, which are capable of providing the power quality, electrical energy storage capacity, and safe dynamic response for on-demand systems in more-electric aircraft. These electrical systems must also reject heat, and they are therefore tightly coupled to thermal system design.

These issues have led the U. S. Air Force to begin a substantial research investment in relevant design approaches, through the auspices of the INVENT program and the energy-optimized aircraft initiatives [1]. A major focus of this research investment has been to develop time-accurate simulations of power and thermal systems to account for potentially unsafe transient behavior as well as mission performance optimality [2]. Work is also progressing on Second-Law methods to determine whether assumed or required heat transfers can occur, particularly in transient contexts [3]. The advantages of exergy-based formulations that combine First-Law and Second-Law formalism have been shown by Doty, Camberos, and Moorhouse [4, 5], and the approach has been applied to aircraft thermal systems by Figliolia, *et. al.* [6]. However, past modeling methods used in industry have been based primarily on steady-state First Law methods exercised over a discrete set of "points in the sky" in aircraft Mach/altitude mission space.

In this project, we develop a MATLAB-based model of a relatively simple, yet representative, aircraft thermal architecture and investigate the parametric design space. This exploration is conducted using a statistical design of experiments (DOE) to sample the design space and parallel coordinates for filtering infeasible designs and determining characteristics of optimal systems. Artificial neural network surrogate models are fit to the DOE results from the MATLAB model in order to reduce the run time and to allow instantaneous interactive graphical filtering by adjusting sliders to alter the parallel coordinates view. This capability extends the traditional role of parallel coordinates as filters on a fixed set of designs to allow new designs to be generated instantaneously and explored to fulfill specific constraints and optimality requirements desired by the user.

Thermal System Model

The thermal system model investigated in this project is shown in Figure 1. The model consists of the following subsystems and components:

- Propulsion system
  - Inlet
  - Fan
  - Heat exchanger to transfer ECS heat to the fan path
  - Compressor
  - Splitter for compressor bleed air
  - Combustor
  - Turbine
  - Core nozzle
  - Fan nozzle
- Fuel thermal system
  - Fuel tank
  - Heat exchanger for ECS loads to fuel
  - Heat exchanger for all other loads to fuel, e.g. oil cooling, hydraulic cooling
  - Splitter for fuel recirculation
- Air-cycle refrigeration system
  - Heat exchanger for bleed air cooling
  - Heat exchanger to transfer ECS heat to fuel
  - Heat exchanger to transfer ECS heat to the fan path
  - Compressor
  - Turbine for power extraction from bleed air
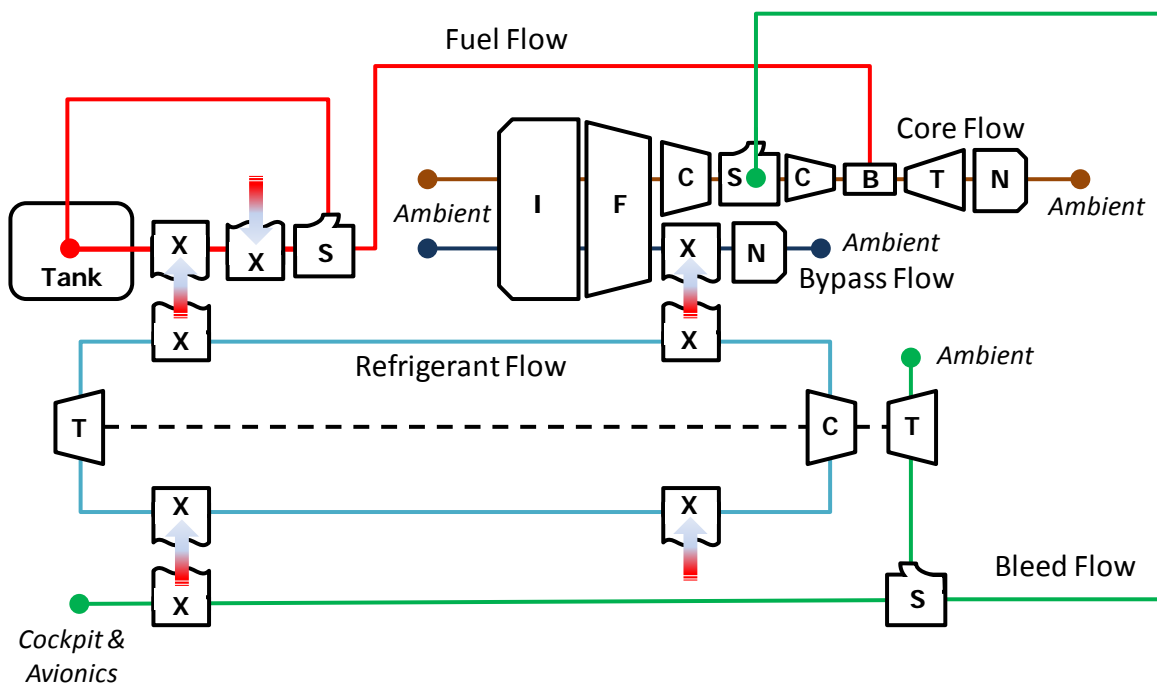 - Turbine for refrigeration cycle cooling

Figure 1: Block diagram of thermal management system model

Engine Model

The propulsion system modeled is a low-bypass ratio separate flow turbofan (SFTF). Although most military engines of interest are mixed-flow turbofans (MFTFs) or variable cycle engines, the separate flow architecture was chosen for this pilot study because of its simplicity. Unlike an MFTF system, an SFTF cycle can be solved directly without iterative loops to balance the fan and core streams in a mixer. Other than the interstage compressor bleed extraction for ECS air delivery, the cycle is presumed to be ideal, i.e. perfect component efficiencies, negligible fuel fraction, and a calorically perfect gas model are specified.

The cycle is modeled through on-design analysis conducted at a supersonic cruise operating condition representative of a modern fighter aircraft. In the thermal system trade studies, the engine cycle design variables are presumed to be fixed at the values shown in Table 1. This approach is generally reflective of the scenario of selecting an "off-the-shelf" engine and designing a thermal management system based on the chosen engine and airframe designs. Engine performance is affected by the thermal system through two mechanisms: (1) ECS bleed extraction from the compressor deteriorates engine TSFC and thrust performance, (2) refrigeration system heat rejection into the fan path improves engine TSFC and thrust performance. Neither the beneficial increase in fuel heating value associated with fuel temperature rise nor the detrimental effects of total pressure drop across the fan path heat exchanger are modeled. Although varying the bleed extraction from an existing engine would in reality reduce not only mass flows but also compressor pressure ratio because of compressor/turbine matching, the pressure ratio is kept at the nominal value in this study. This approach reduces the complexity of the engine model considerably and is an appropriate approximation for small variations in the bleed extraction.

Table 1: Engine Cycle Definition

Variable	Value	Units
Mach number	1.2	--
Ambient temperature	420	°R
Ambient pressure	6.5	psi
Fan Pressure Ratio	1.5	--
Overall Pressure Ratio	28	--
Bypass Ratio	0.6	--
Turbine Inlet Temperature	3000	°R

Fuel Thermal System Model

The fuel thermal system is modeled as a simple feed circuit from the tank, passing through two heat exchangers, and then to the engine. The first heat exchanger in the flow path accepts heat from the refrigeration system and transfers it to the fuel. In some architectures, this heat transfer is accomplished through an intermediate polyalphaolefin (PAO) loop, but this loop in not directly modeled in the architecture developed for this project.

The second heat exchanger accepts all additional heat transferred to the fuel from airframe and engine systems. Whereas most architectures employ multiple heat exchangers for each fuel thermal load, e.g. oil and hydraulics, the second heat exchanger in this model can be interpreted as a series combination these various exchangers and sources.

Fuel recirculation is modeled by considering fuel temperature limits in the heat exchangers (due to load constraints or fuel thermal stability). If the engine fuel demand results in inadequate heat transfer based on this maximum fuel temperature, additional fuel is flowed through the heat exchangers and then routed through a recirculation circuit. The fuel temperature limit modeled in this study is held constant at 595°R.

The fuel thermal model developed for this project is not integrated in time throughout an aircraft mission to track the rise in fuel tank temperature, as was conducted in the recent paper by the German [7]. Instead, fuel tank temperature is treated as a variable that can be changed in design studies to simulate differing operational conditions at specific points during a mission.

Refrigeration System Model

The ECS refrigeration system is modeled as a "reverse Brayton" refrigeration cycle. The working fluid is air, and the cycle is closed. The purpose of the system is to refrigerate engine bleed air that is to be provided to the cockpit and to the avionics bay.

The architecture consists of a power turbine fed by a fraction of the engine compressor bleed air, a turbine for expansion of the refrigerant fluid, a compressor for the refrigerant, and three heat exchangers. The primary heat exchanger accepts heat from the compressor bleed flow and provides the cooling needed for the ECS system. The other heat exchangers reject heat from the refrigeration cycle to the fuel and to the propulsion system fan flow path.

Implementation

Models of the systems described in the sections above were implemented in MATLAB using and object-oriented approach. This allows thermodynamic systems to be rapidly modeled and modified. Each physical component of the system is modeled as an object with properties that encode the component's design parameters and an inlet and outlet port (or multiple outlet ports in the case of a splitter component). The components are linked by flow objects, which link the outlet port of one component to the inlet port of the next component in the system. The flow objects have properties that encode the thermodynamic state variables and mass flow rate and velocity. The net heat or work of a particular component can be calculated by comparing the change in the values of the state variables across the component, or alternatively, the net heat or work can be specified directly and a related physical parameter of the component can be calculated as a dependent variable. For example, the net work of a turbine can be specified to calculate the corresponding pressure across the turbine. For simplicity, all fluids are modeled with constant heat capacities.

Exploration of the Multi-Variate Design Space

Two studies were conducted to examine the implications of differing approaches to thermal system modeling. In the first study, the heat transfer between the two flows in each heat exchanger is directly specified as an independent variable. In the second study, the heat transfer in each heat exchanger is calculated as a function of the inlet temperature of each flow and the heat exchanger's effectiveness – a scalar parameter between 0 and 1 that encodes the heat

exchanger's flow architecture, material properties, and size. Consequently, each study has a different set of independent and dependent variables, but the design objectives in each case remain the same: to design a feasible thermal management system that minimally degrades engine performance.

In these studies, feasibility is determined by two types of constraints. First, the system must be physically realizable. This is checked by calculating the exergy destruction across the three heat exchangers in the Air Cycle Refrigeration system with feasibility corresponding to net exergy destruction. Second, the final temperature of the ECS air must be between 400°R and 460°R. The upper temperature limit ensures that the ECS air is cold enough to cool the cockpit and air-cooled avionics, while the lower temperature limit filters out over-designed refrigeration cycles. Systems that demonstrate optimal performance are those that meet all feasibility constraints and produce the lowest values of TSFC and least degradation of engine thrust.

Study 1: Direct Specification of Thermal Loads

The independent variables for Study 1and their allowable ranges are listed in Table 2, and the dependent variables are listed in Table 3.

Table 2: Independent variables and their ranges for sampling of the design space for Study 1

Description	Variable Name	Min	Max	Units
Refrigeration system compressor pressure ratio	PRrefrig	4	12	--
Fuel tank temperature	Tfuel	460	560	°R
Refrigeration system reference pressure	P_refrig	5	50	psi
Avionics heat load	load_Avionics	5000	10000	ft-lb/s
Fuel heat load from non-ECS sources	load_Fuel	100000	200000	ft-lb/s
ECS heat load	Qdot_ECSHX	100000	170000	ft-lb/s
Fan path exchanger heat load	Qdot_FanHX	140000	180000	ft-lb/s
Fuel heat load from refrigeration system	Qdot_FuelHX	40000	130000	ft-lb/s

Table 3: Dependent variables for Study 1

Description	Variable Name	Units
Exergy creation in the ECS heat exchanger	dX_ECSHX	ft-lb/s
Exergy creation in the fan heat exchanger	dX_FanHX	ft-lb/s
Exergy creation in the fuel/refrigeration loop heat exchanger	dX_FuelHX	ft-lb/s
Temperature feasibility check in the ECS heat exchanger	check_ECSHX	--
Temperature feasibility check in the fan heat exchanger	check_FanHX	--
Temperature feasibility check in the fuel/refrigeation loop heat exchanger	check_FuelHX	--
Thrust	Thrust	lb
Recirculated fuel flow rate	recircFuelFlow	slug/s
Bleed flow delivery temperature to ECS	T_ECS	°R

The design space described in Table 2 was sampled using a 1000 point Latin Hypercube (space filling) designed experiment. Each of the 1000 points was evaluated using the object oriented thermal system model in MATLAB. The resulting values were used in Rave to create the figures shown below.

Parallel coordinates plots were employed because of their effectiveness for viewing the entire design space in a single graphic. In these plots, each variable of interest is plotted on one of a series of equal-length, parallel coordinate axes. A single design is represented by a polyline that connects the points on the axes corresponding to its design parameters and performance.

An example parallel coordinates graph is presented as Figure 2, which shows all 1000 designs that were sampled. Each polyline is plotted in a slightly different shade of blue to help the viewer more easily distinguish the individual lines. Several important visual effects of parallel coordinates graphs can be observed. Experienced users learn to account for these effects in judging a parallel coordinates plot, but the effects may mislead users who are not acquainted with these types of graphics.

The first observation is that tradeoffs between adjacent variables can be judged by comparing the slopes of the line segments between the axes. Small slopes (horizontal or nearly horizontal line segments) indicate positive correlation, while large slopes (either positive or negative slopes) indicate an inverse correlation relationship.

The second important observation involves the apparent distribution of data. Because the length of each line segment depends on the relative coordinates along each axis, lines of strong inverse correlation are longer than lines of strong positive correlation. This creates a visual effect in which negative correlations may seem evident when in fact the variables are uncorrelated. An example can be seen in the line segments connecting Qdot_ECSHX and Qdot_FanHX in Figure 2. These two variables are uncorrelated, but there is a strong visual "X" pattern that might suggest a negative correlation. This effect can be compared with the segments between dX_ECSHX and dX_FanHX, which are in fact negatively correlated. Note in this second case how deep "V" shaped gaps appear at the top and bottom of the plot. These are a more reliable indicator of tradeoff between variables.

Lastly, this effect also causes the distribution of points along any single axis to appear to be more clustered toward the extreme values. This effect is illusory and not reflective of the true point distribution. For example, the points along any of the three Qdot axes appear clustered toward the end points (high or low values) with fewer points near the center of the axis, while the distribution of points along the dX_ECSHX axis appears to be more uniform. In reality, the Qdot variables are uniformly distributed throughout their range, while dX_ECSHX is approximately normally distributed.
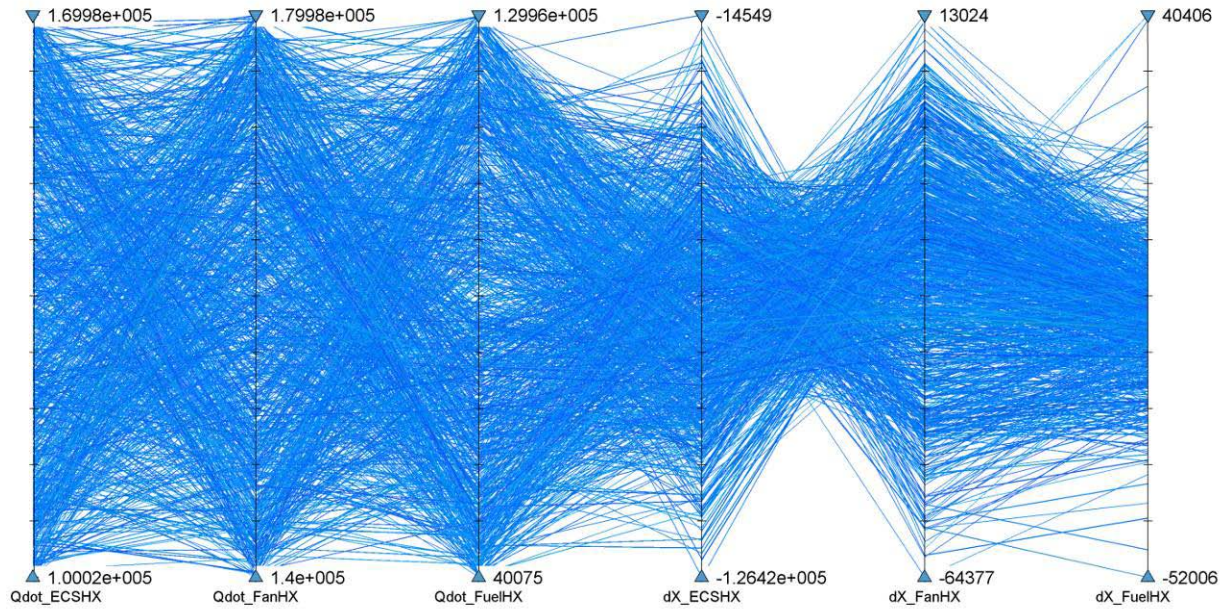
Figure 2: Parallel coordinates plot of heat transfer and change in exergy in the three Air Cycle heat exchangers

While Figure 2 shows some general tradeoffs between the heat transfers in each heat exchanger and the corresponding changes in exergy, it also contains many infeasible designs that obfuscate the relevant design trends. These infeasible designs can be removed by filtering.

First, we filter out designs that have a positive change in exergy (an exergy creation) for any of the heat exchangers. The variables dX_ECSHX, dX_FanXH and dX_FuelHX represent the net change in exergy of the flows in each heat exchanger in steady state operation, calculated using control volumes that surround each heat exchanger. Since the change in exergy for these control volumes must be negative in order to be physically possible, designs in which any of these variables have a value greater than 0 are filtered. This is accomplished by interactively sliding the triangular filter down the axis to the "0" value. The resulting filtered plot is shown in Figure 3.

While this filter effectively removes many infeasible designs, careful examination of the results reveals that several infeasible designs remained unfiltered. The reason for their exclusion is explained in Figure 4. By considering the control volume around the entire heat exchanger, it is possible that a region of the heat exchanger violates the exergy destruction principle, but the exergy created is "canceled out" by the much greater exergy destruction elsewhere in the heat exchanger. The exchanger as a whole then appears to obey the exergy destruction principle.
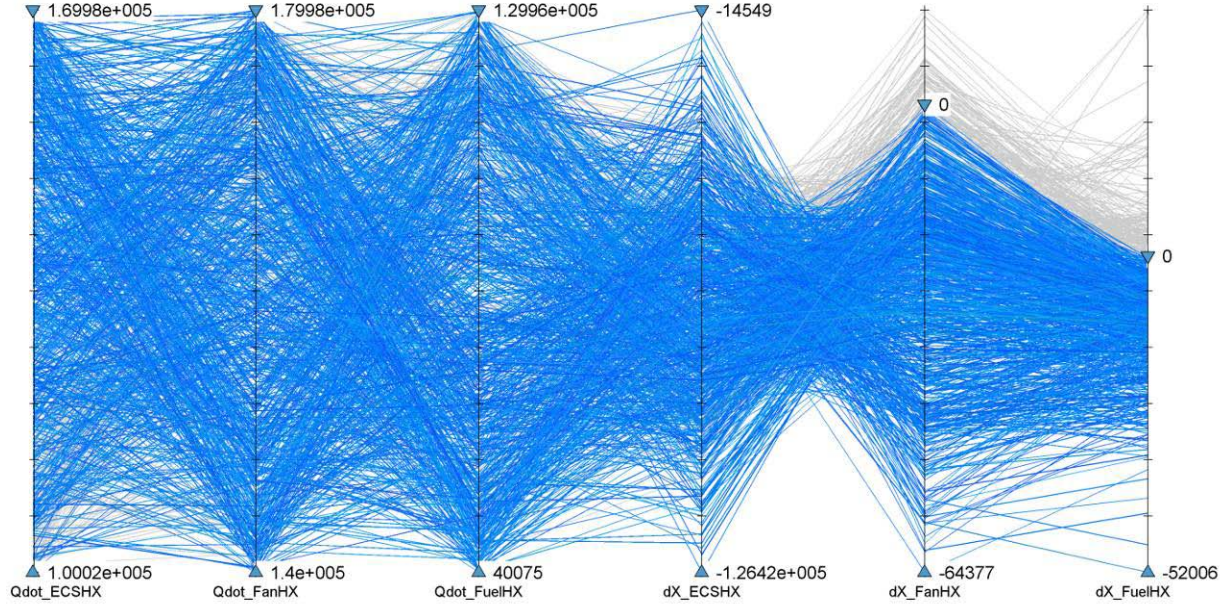
Figure 3: Filtering on the constraint the dX<0 removes several infeasible designs (shown in gray)

This situation implies that when treating the entire heat exchanger as a lumped element, there is a need to consider not only exergy creation but also the bounding hot and cold stream temperatures. To account for this consideration in our model, three additional "check" variables were added. These variables are formulated to indicate if part of the heat exchanger violates the exergy destruction principle (value = 0) or if the entire heat exchanger is feasible (value = 1) by comparing inlet and outlet temperatures of the hot and cold flows.
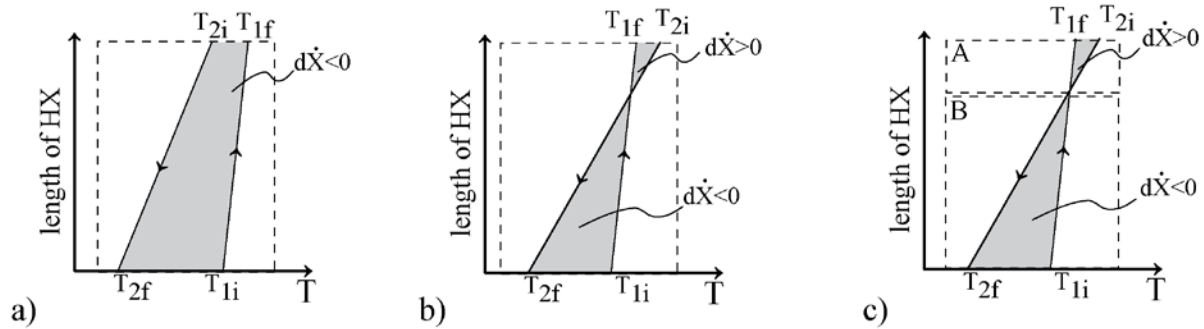
Figure 4: Exergy changes in counter flow heat exchangers. Subscript 1 indicates hot flow, Subscript 2 indicates cold flow. Dashed lines indicate system boundary. a) Real heat exchanger – exergy is destroyed. b) Impossible heat exchanger that involves heat transfer from low temperature to high temperature within a portion of the exchanger; however the system as a whole still demonstrates net exergy destruction. c) By dividing the heat exchanger into two systems, System A has net exergy creation, revealing impossibility.

Figure 5 shows the parallel coordinates plot that has been expanded to include these three additional variables with the filters set to remove infeasible designs as defined by check variable values equal to zero. Comparing the location of the filtered designs on the dX_FanHX and

dX_FuelHX axes confirms the explanation above: even heat exchangers with some net exergy destruction, as measured for the entire heat exchanger control volume, are actually infeasible. This occurrence emphasizes the importance of intelligently choosing the control volume to be analyzed. It is also interesting to note that only a single design failed the ECS heat exchanger check and to observe the resulting visual effect between the dX_FuelHX and check_ECSHX axes in Figure 5.
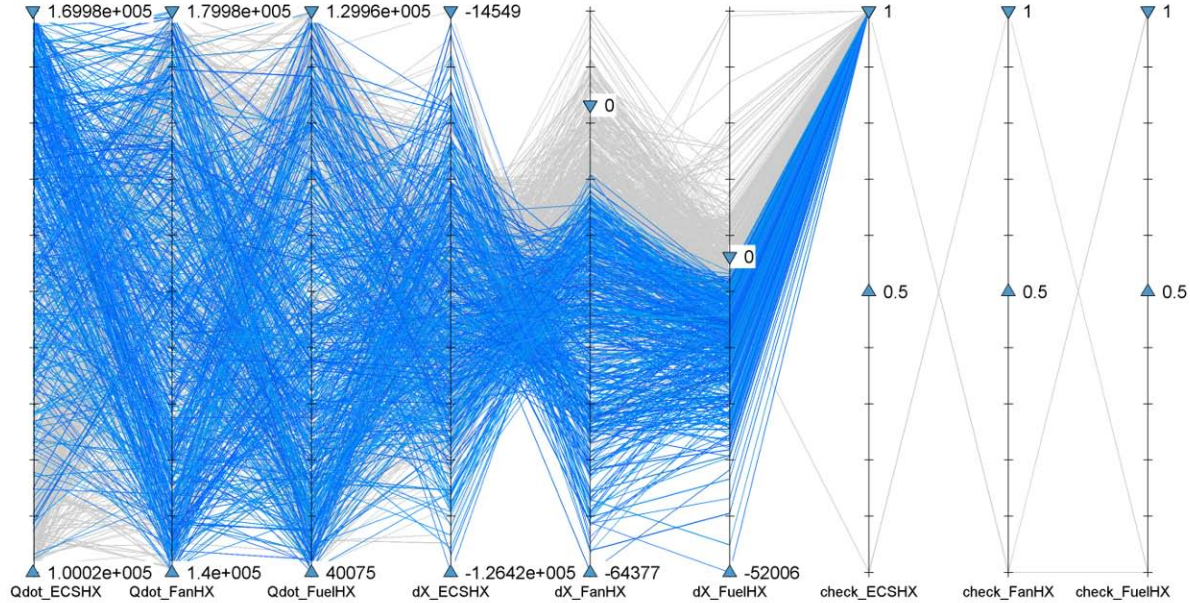

Figure 5: Filtering on the heat exchanger "check" variables removes additional infeasible designs. Note the location of the labeled 0 values of dX_FanHX and dX_FuelHX

We next filter designs that result in ECS air temperatures outside of an allowable range of 400°R to 460°R. As shown in Figure 6, this filter removes many more infeasible points, and clearly reveals a much smaller range of Qdot_ECSHX that contains all of the feasible designs.

Having filtered all infeasible designs, attention is turned to the relation between the independent variables and the performance metrics. Figure 7 shows the parallel coordinates plot when the cycle parameter variables are included. For clarity, the Qdot, dX, and "check" variables have been removed from the plot, though their filters are still enforced. Additionally, the lines in Figure 8 are colored according to the value of thrust. This color coding simplifies the comparison of trends between any variable and thrust, regardless of the order in which the variables are arranged in the plot. It is immediately apparent that high thrust corresponds to low PRrefrig, and also that changes in thrust are inversely proportional to changes in TSFC. These trends directly reveal the influence of the refrigeration cycle on engine performance: Higher refrigeration pressure ratios require additional work extraction from the engine, resulting in reduced engine thrust and increased fuel burn. Weaker trends show that high thrust corresponds to high Tfuel and low recircFuelFlow, although at least a few points contradict these general trends.
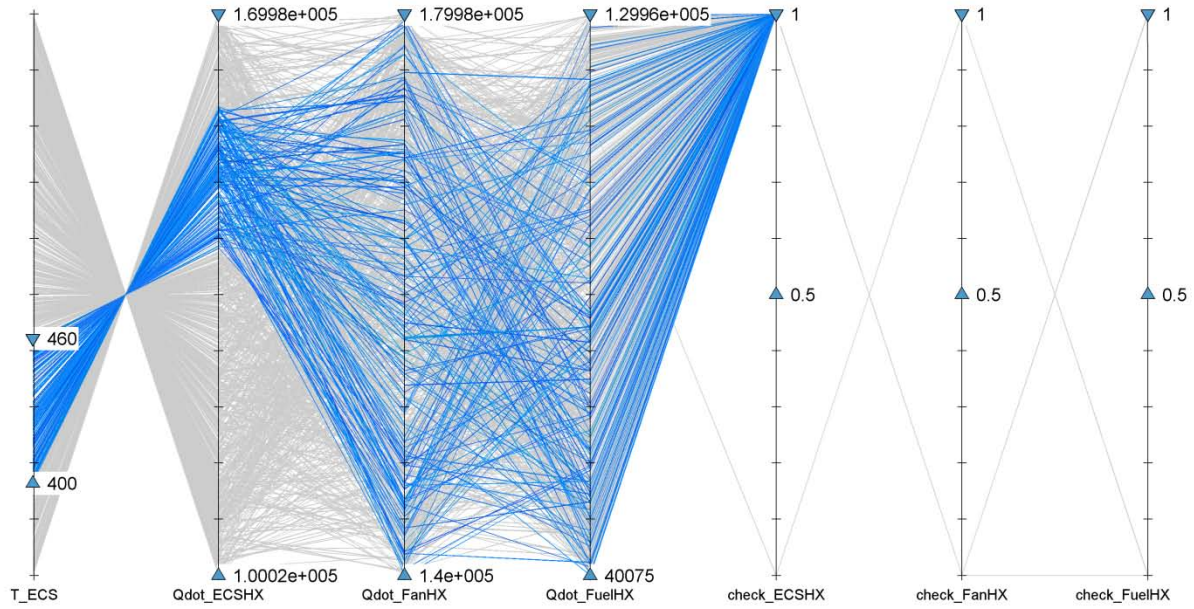
Figure 6: Filtering on the temperature requirement of the ECS air removes many more infeasible designs.
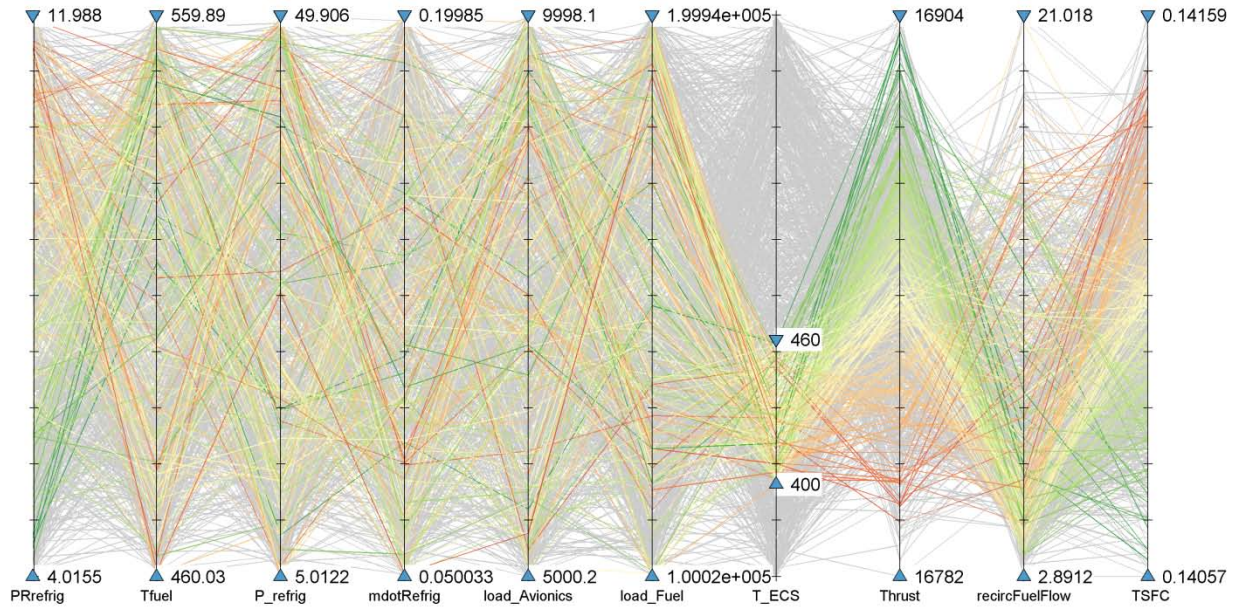

Figure 7: Parallel coordinates plot of independent variables with performance metrics. Color-coding lines enables comparisons to be easily made across all variables. Here, coloring by Thrust reveals a relationship with PRrefrig.

In Figure 8, the lines are colored according to the value of recircFuelFlow. The most obvious dependency is between recircFuelFlow and Tfuel, with the expected results that colder fuel requires less recirculation because a given mass of cold fuel can receive more heat before reaching its limiting temperature. A weaker trend suggests that it is desirable to maximize PRrefrig and P_refrig. Note that there are more green lines than red lines in Figure 8 because the feasible designs are primarily clustered around low values of recircFuelFlow.
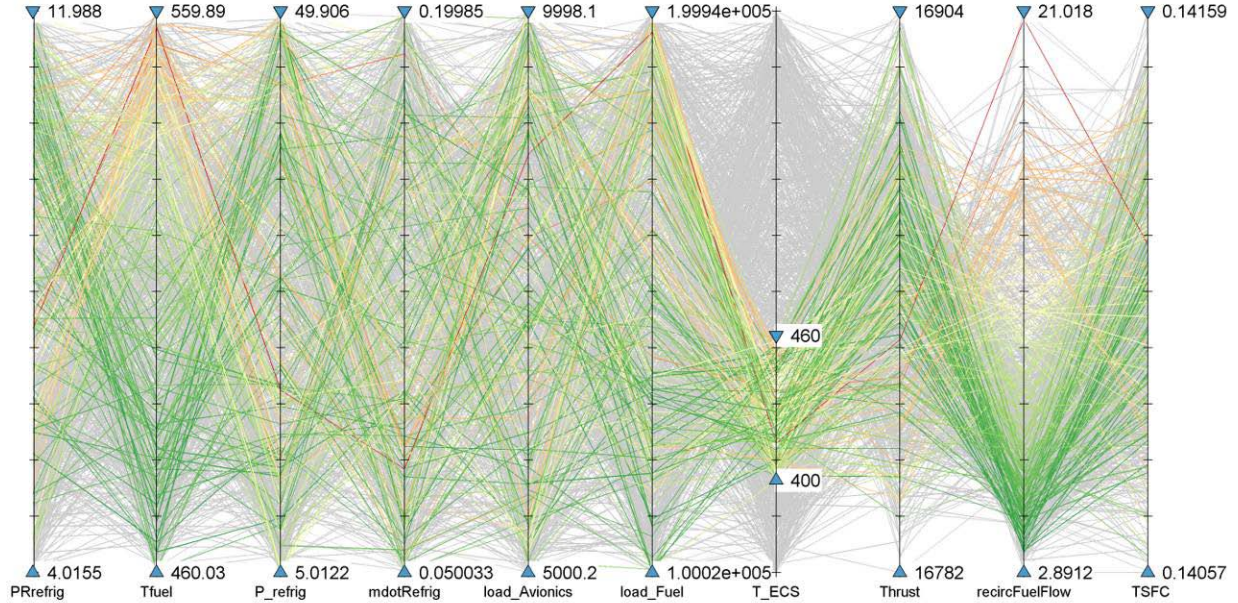

Figure 8: Coloring by recircFuelFlow reveals a strong relationship with Tfuel, and weaker relationships with PRrefrig and P_refrig.

Further exploration of the design space can benefit from "locking in" some of the independent variables at fixed values that are deemed to be good. The reduced-dimensional design space can then be explored interactively by changing these fixed values (by using a slider bar) and watching the animated effect that the changes have on the parallel coordinates plots. In order to enable this capability, the parallel coordinates plot must be able to communicate directly with the system model in order to determine the results corresponding to arbitrary design variable settings. Traditional parallel coordinates implementations do not have this capability, as they only plot results from a static data set such as a DOE. This functionality therefore requires a new parallel coordinates formulation. This functionality was developed in the Rave software as a part of this project.

The operation of "locking in" design variables is computationally intensive, requiring that each of the 1000 designs be recalculated by calls to the computational model each time one of the "locked in" values is changed. The object-oriented thermal system model can evaluate approximately five designs per second on a modern desktop PC. Consequently it takes several minutes to evaluate all 1000 designs. In order to speed up the evaluation to allow interactive design space exploration, neural network approximations of the object oriented model were created. The accuracy of these approximations is illustrated in Figure 9. The vertical axis of each plot, the residual, is the difference between the value calculated by the neural network (the

"predicted" value) and the value calculated by the object-oriented model. The residuals are orders of magnitude smaller than the values, indicating highly accurate approximations. An additional neural network was created to encode all of the feasibility checks into a single variable, named "isFeasible." The accuracy of this discrete-valued neural network is assessed by calculating the percentage of designs that it correctly identifies as feasible or infeasible. This value was found to be 97.2%, again indicating a highly accurate approximation. As shown in Figure 9, the regressions show some patterns in the residuals, indicating the presence of some degree of higher-order effects that are not modeled. However, the variations in the residual have a small magnitude and the models were deemed adequately representative for this demonstration study.
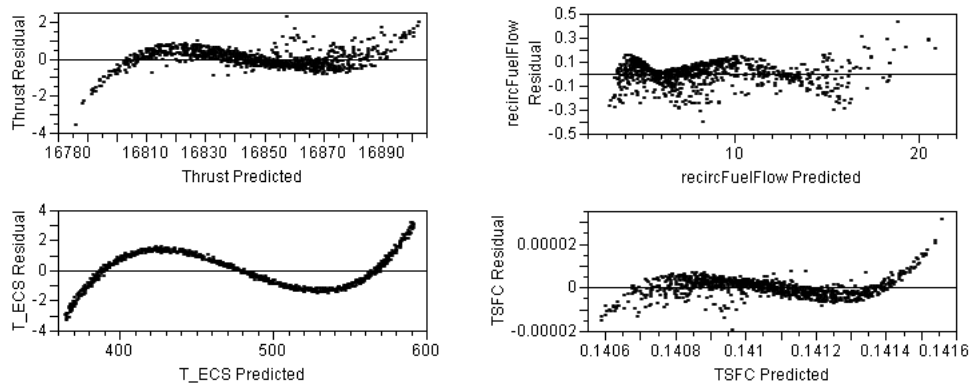

Figure 9: Residual plots of artificial neural network approximations of the four performance variables for Study 1

By using these neural networks, all 1000 designs can be evaluated in a fraction of a second, thus allowing nearly instantaneous recalculation of the parallel coordinates plot. Figures 10 and 11 show the effect of locking in PRrefrig at a particular value, while all other design variables are held at the values prescribed by the Latin hypercube designed experiment. It can be seen that when PRrefrig is locked in at a low value, TSFC is generally low and thrust is generally high. When PRrefrig is increased, TSFC rises and thrust drops. When used interactively on a computer, the user can slide PRrefrig along its axis and the polylines update instantly to reflect the impacts of the locked in value.

In the extreme, the user could lock in values for all of the independent variables, so that the parallel coordinates plot shows only a single polyline connecting the locked in values and the corresponding values of the dependent variables. However, in doing so, a problem arises: the strength of the parallel coordinates plot is that by plotting many designs the user can infer relationships between the variables. With only a single polyline plotted, relationships cannot be inferred and it becomes difficult to predict the effects that changing the locked in values has on the dependent variables.

To overcome these conflicting needs – the need to reduce the extent of the design space and the need to understand the effects of changing independent variables – the parallel coordinates graph is paired with another type of plot, a "prediction profiler." A prediction profiler, an example of which is shown in Figure 12, consists of a matrix of axes, each of which plots the univariate relationship between one independent variable and one dependent variable.
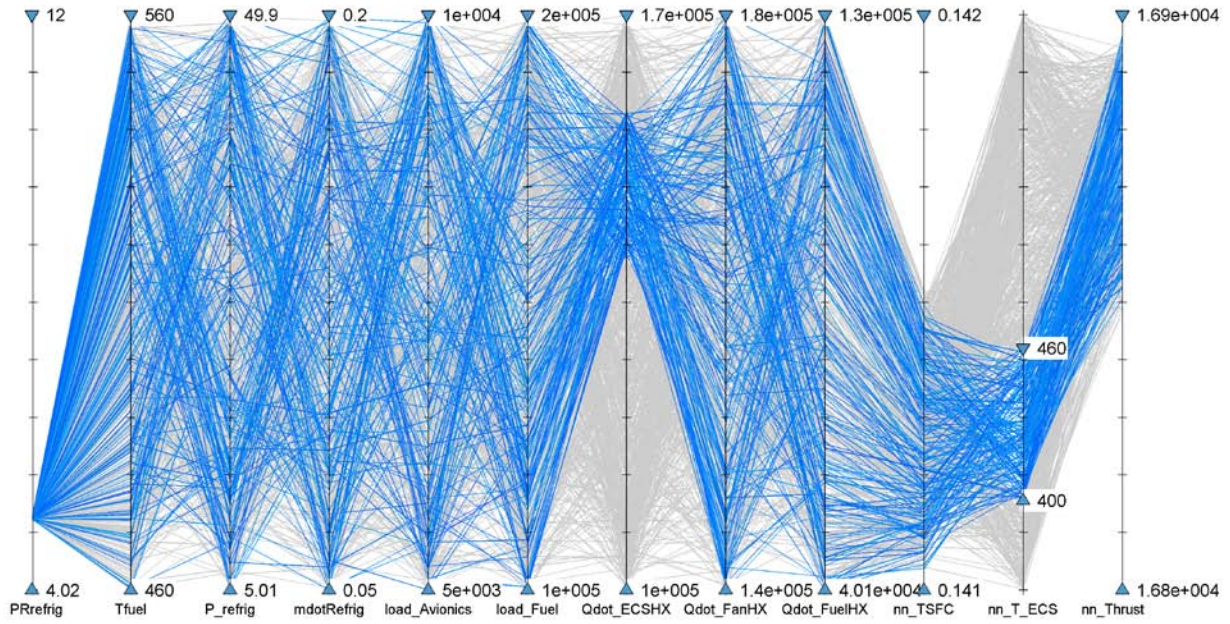
15

Figure 10: Locking PRrefrig at a low value results in high values of Thrust and low TSFC
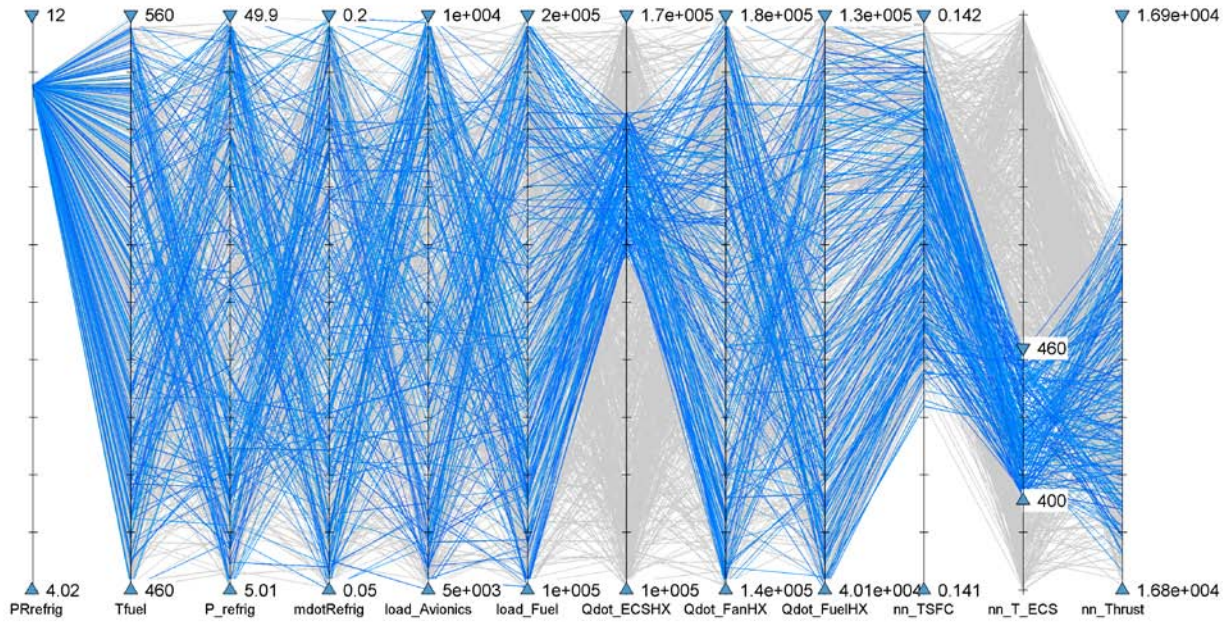

Figure 11: Locking PRrefrig at a high value results in low values of Thrust and high TSFC
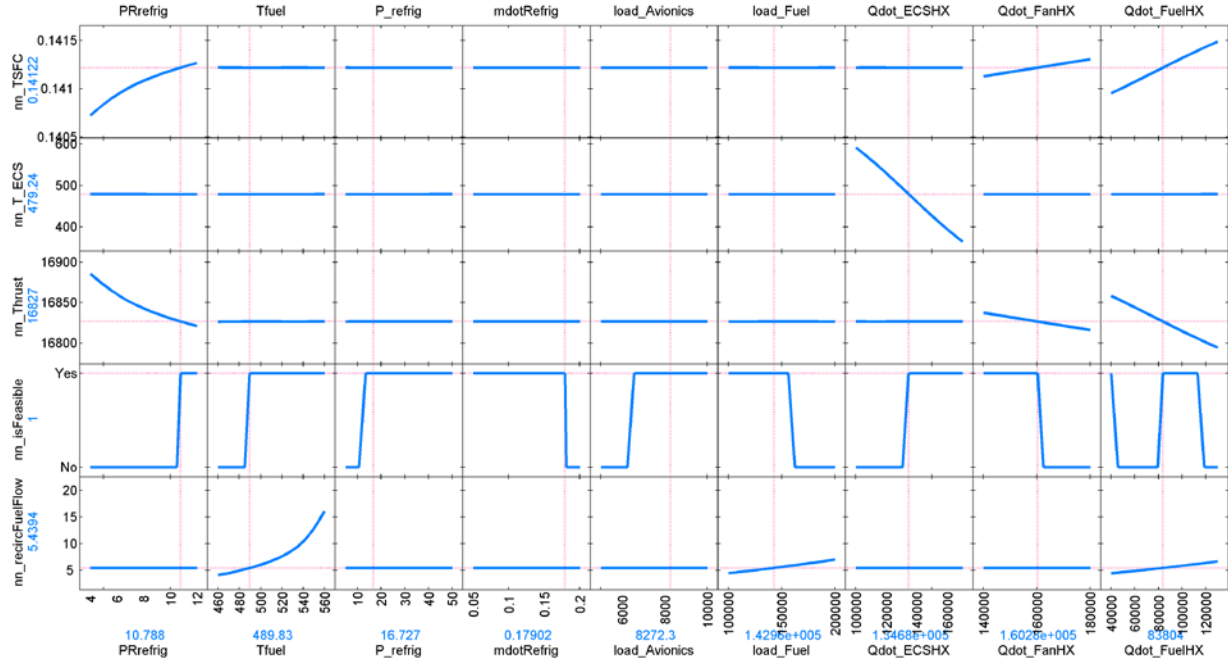
Figure 12: Prediction profiler reveals effects of independent variables on feasibility and the four performance metrics. Independent variables are listed along the horizontal, dependent variables along the vertical. Each blue curve shows the univariate relationship between one independent variable and one dependent variable while all other dependent variables are held constant at the values indicated by the vertical magenta lines. A prediction profiler is a type of multi-dimensional sensitivity matrix plot.

The prediction profile thus explicitly displays the effects of changing independent variables, with the caveat that it shows this information as it is calculated at a single point in the design space. At a different point in the design space, the effects might be quite different. Consequently, the prediction profiler shows a *local* view of the design space, while the parallel coordinates plot shows a *global* view of the design space.

By examining the prediction profiler in Figure 12, it can be seen that relatively few of the independent variables affect the values of the dependent variables relevant for optimization; however, all of them affect feasibility in some way. In Study 2 we will consider a more sophisticated heat transfer model that has more complex relationships between the independent and dependent variables.

Study 2: Specification of Heat Exchanger Effectiveness

In Study 1, heat transfer rates were specified independently without regard to temperatures of the hot and cold flows. The result of this approach was that many of the designs sampled in the DOE were infeasible, as indicated by exergy creation and/or violations of the temperature condition "check variables." Although this method results in a greater number of infeasible designs, the advantage of the approach is the simplicity of the heat transfer formulation, i.e. the heat exchanger design properties do not need to be specified. As shown in the Study 1, these

17

designs can be filtered based on exergy and the temperature check variables to determine the feasible subset.

An alternate approach is to specify heat exchanger parameters directly such that heat flows become dependent variables based on the heat exchanger properties and bounding temperatures. In Study 2, heat transfer is calculated with this more sophisticated heat exchanger model.

To formulate this approach, the heat exchange is modeled through the effectiveness-NTU method. The heat transfer is calculated as,

$$\dot{Q} = \varepsilon \, C_{\min} \left(T_{n,\,in} - T_{c,\,in} \right)$$

where $T_{h,\,in}$ is the entrance temperature of the hot flow, $T_{c,\,in}$ is the entrance temperature of the cold flow, ε is the effectiveness of the heat exchanger, and $C_{\min} = \min\left[\left(\dot{m}\,c_p \right)_h, \left(\dot{m}\,c_p \right)_c \right]$ is the minimum heat capacity rate of the hot and cold flows, respectively. The effectiveness, ε, is a function of the heat exchanger area and type (cross-flow, counter-flow, etc.) and the minimum and maximum heat capacity rates of the two flows [8]. Effectiveness can, in principle, take values between zero and one, but the maximum practical values depend on the heat exchanger architecture. Values between 0.5 and 0.9 represent a typical range for most well-designed exchangers and operating profiles.

The independent variables for Study 2 and their ranges are listed in Table 4. As in Study 1, these ranges were sampled in a 1000 point Latin hypercube designed experiment to populate the design space.

Table 4: Independent variables and their ranges for sampling of the design space for Study 1

Description	Variable Name	Min	Max	Units
Refrigeration system compressor pressure ratio	PRrefrig	4	12	--
Fuel tank temperature	Tfuel	460	560	°R
Refrigeration system reference pressure	P_refrig	5	50	psi
Avionics heat load	load_Avionics	5000	10000	ft-lb/s
Fuel heat load from non-ECS sources	load_Fuel	100000	200000	ft-lb/s
ECS heat exchanger effectiveness	eta_ECSHX	0.5	0.9	--
Fan path heat exchanger effectiveness	eta_FanHX	0.5	0.9	--
Fuel/refrigeration heat exchanger effectiveness	eta_FuelHX	0.3	0.7	--

Note that the heat exchanger between the refrigeration loop and the fuel has been modeled with a lower efficiency than the other exchangers because it is intended as a simpler representation of a typical architecture that consists of a pair of heat exchangers operating with a PAO loop between the refrigeration cycle and the fuel recirculation cycle. The intermediate PAO loop has not been directly modeled, but the lower effectiveness in this exchanger is intended to simulate the presence of this loop indirectly.

By modeling the heat exchangers using effectiveness values between 0 and 1, it is no longer necessary to check for feasible values of exergy destruction, as feasibility is guaranteed within this range. Instead, we compare the effects of heat exchanger effectiveness on heat transfer and

exergy destruction. The results for each heat exchanger are shown in Figure 13. The ECS heat exchanger is the most straightforward to interpret: high effectiveness leads to high heat transfer, which in turn leads to high exergy destruction (large negative values of dX). The Fan and Fuel heat exchangers are complicated by the fact that they are adjacent to each other in the refrigeration loop, and thus their performances are tightly coupled.
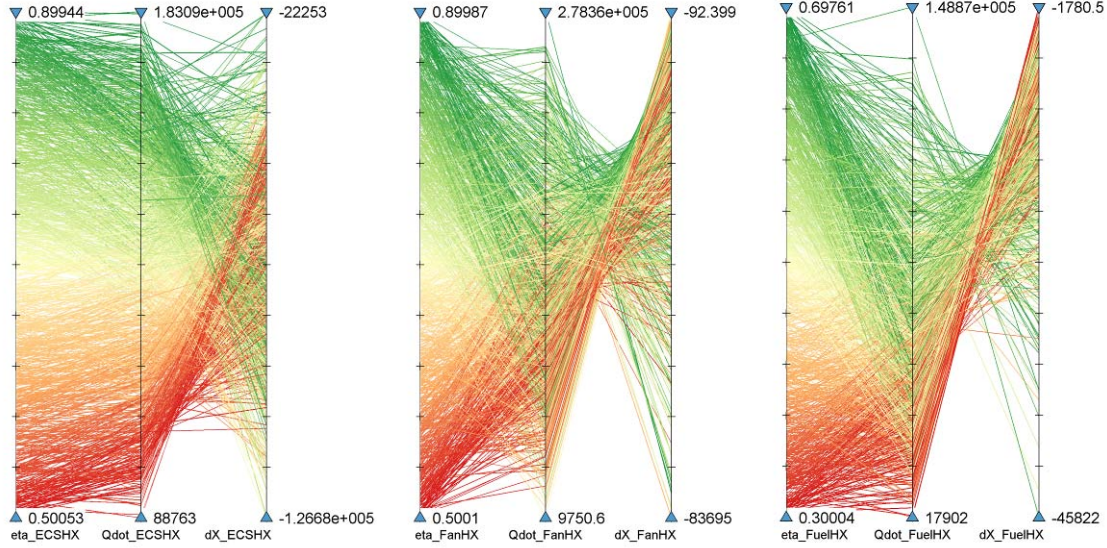

Figure 13: Comparison between effectiveness, heat transfer, and change in exergy for the three Air Cycle heat exchangers

The coupling between the Fan and Fuel heat exchangers is illustrated in Figure 14. It is seen that the effectiveness of the Fan heat exchanger, which the air cycle flow encounters first, has a very strong effect on the heat transferred to the fuel. This is because the inlet temperature to the Fuel heat exchanger depends on the amount of heat transfer in the Fan heat exchanger.
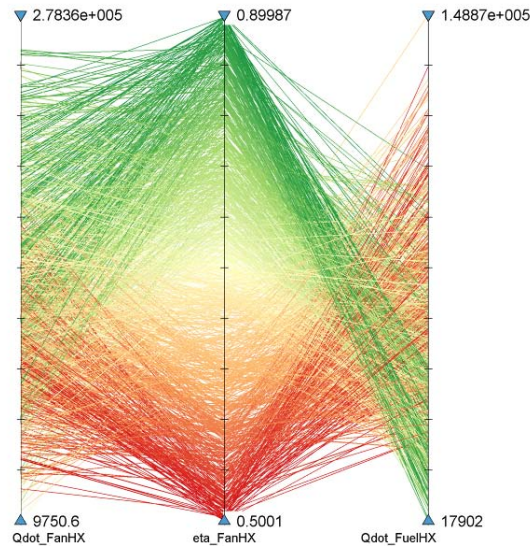

Figure 14: Relationship between Fan Heat Exchanger effectiveness and the heat transfer in the Fan Heat Exchanger and the Fuel Heat Exchanger

Parallel coordinates plots of the full design space are shown in Figures 15 and 16. These plots reveal similar trends to the plots in Figures 10 and 11 from Study 1.
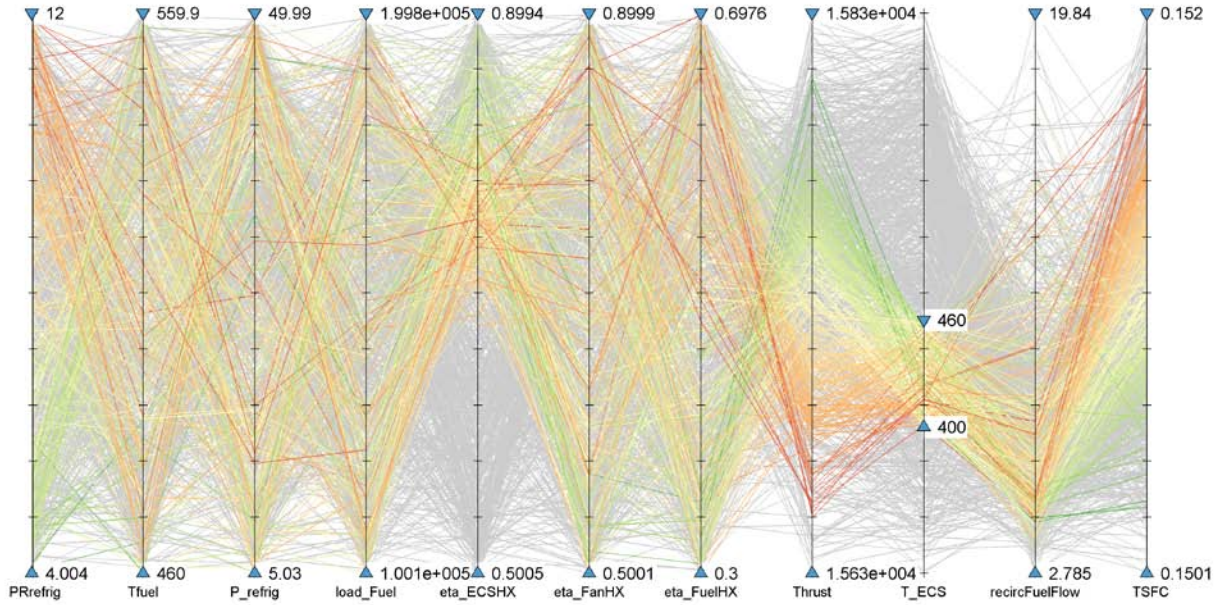

Figure 15: Coloring according to thrust reveals a relationship with PRrefrig (c.f. Figure 8)
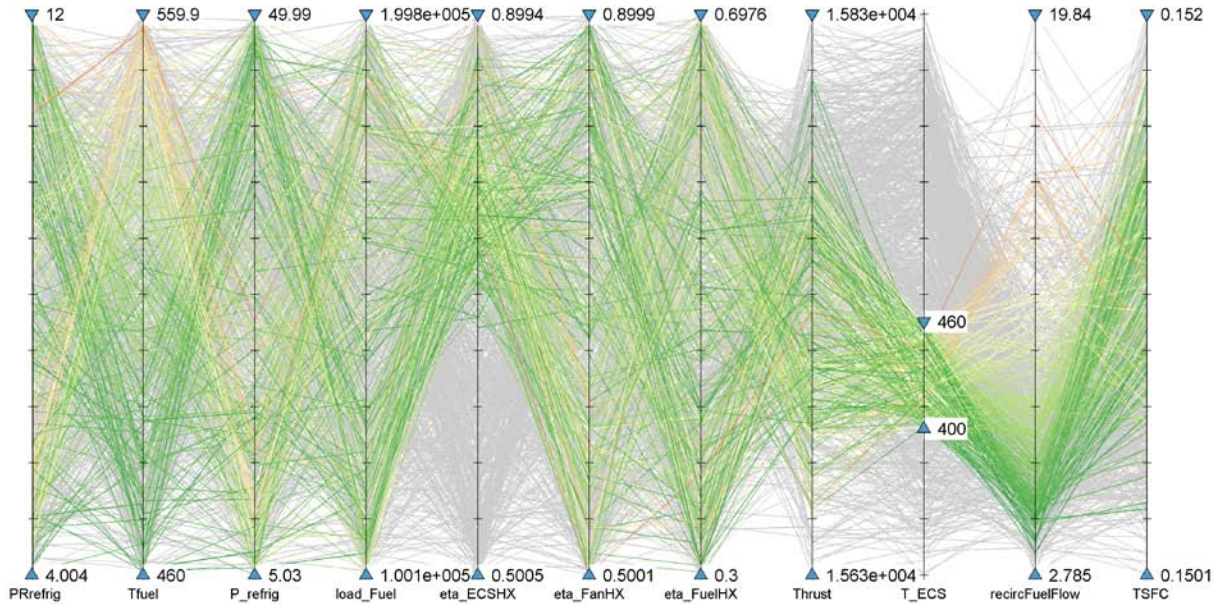

Figure 16: Coloring according to recircFuelFlow reveals a relationship with Tfuel (c.f. Figure 9)

As in Study 1, neural network surrogate models were created to enable interactively "locking in" values for the independent variables. The plots in Figure 17 show the residuals of these fits. The quality of the approximations, as measured by the magnitude of the residuals, is not as favorable

as in Study 1. This is because the thermal system being modeled is now more complex, and thus harder to approximate with a simple algebraic function.

The neural network models were used to create the prediction profiler in Figure 18. Compared to the prediction profiler from Study 1, this profiler shows new relationships between the variables. For example, the mass flow rate of the air cycle is now seen to be an important factor for determining heat transfers and performance metrics. Furthermore, it is seen that the effectiveness of each heat exchanger is an important driver of the performance metrics.

In light of the importance of heat exchanger effectiveness, a study was conducted to examine the effect of locking in values for the heat exchangers on the total variability of the performance metrics. The two parallel coordinates plots in Figures 19 and 20 are representative of the results. In these plots, the effectiveness of each heat exchanger has been locked in at a single value, while the remaining independent variables vary randomly within their ranges according to the Latin hypercube designed experiment. In Figures 19 and 20, the *difference* between the ranges spanned by each dependent variable is indicative of the effect of changing the effectiveness of the ECS heat exchanger. The extent of the range spanned by each dependent variable in either Figure 19 or 20 is indicative of the variability in the dependent variables due to variability in the unplotted (not locked-in) independent variables.
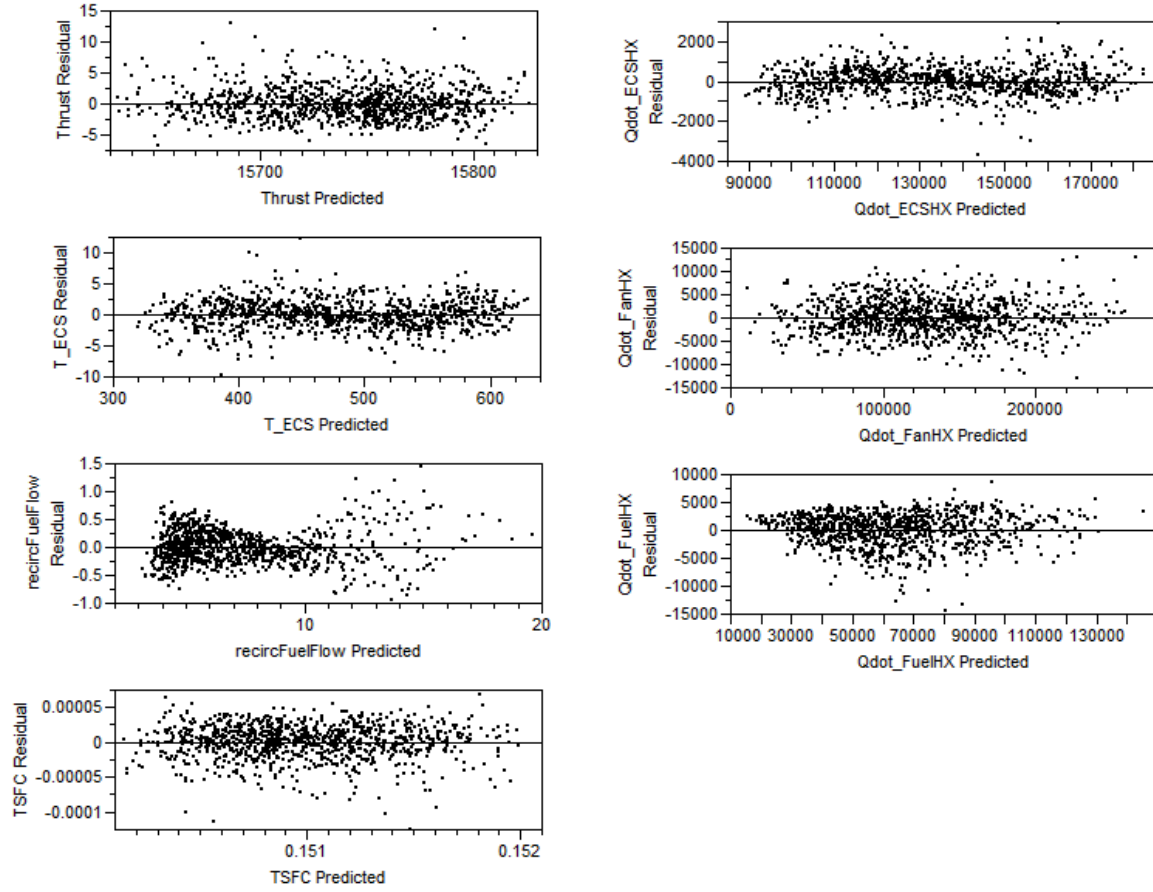
Figure 17: Residual plots of artificial neural network approximations of the performance variables and heat exchanges for Study 2. (c.f. Figure 10)
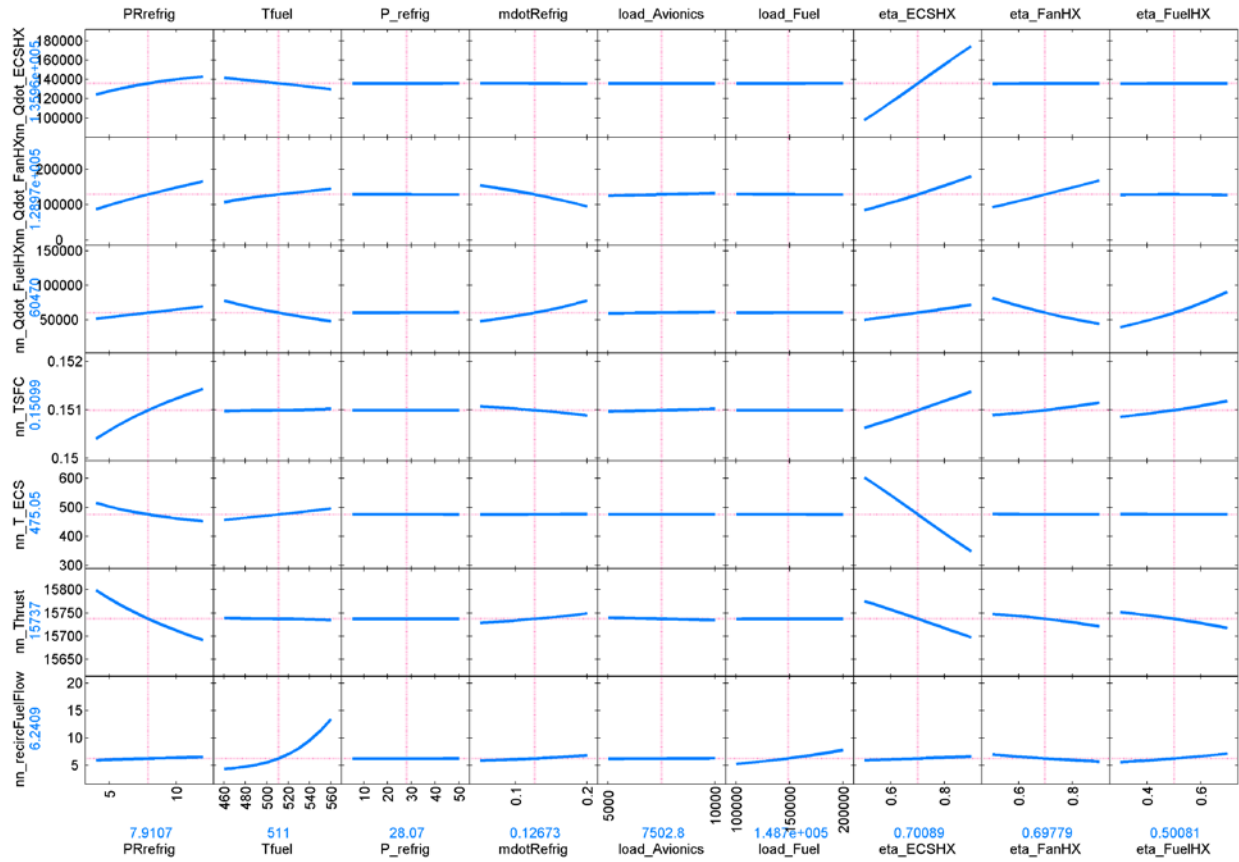
Figure 18: Prediction profiler for Study 2. (c.f. Figure 13) Compared to Study 1, more effects can be seen here, indicating the greater complexity of the model in Study 2. The effectiveness of the ECS Heat Exchanger is seen to be the most influential variable
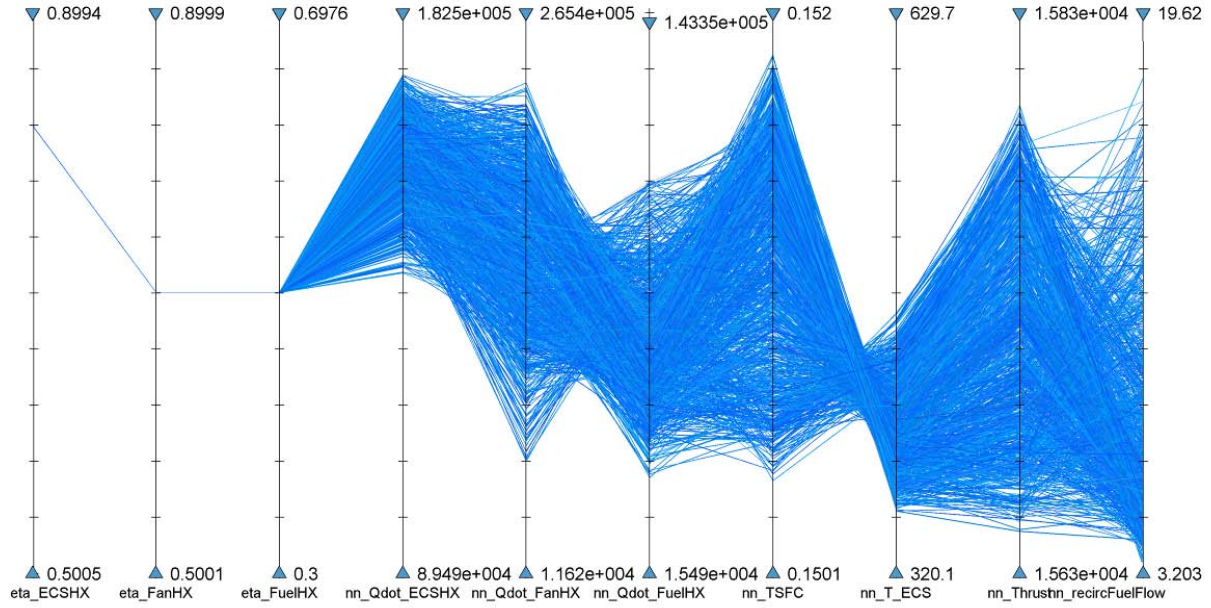
23

Figure 19: Parallel coordinates plot with each heat exchanger's effectiveness locked at a constant value while the remaining independent variables (unplotted) vary within their full allowable range
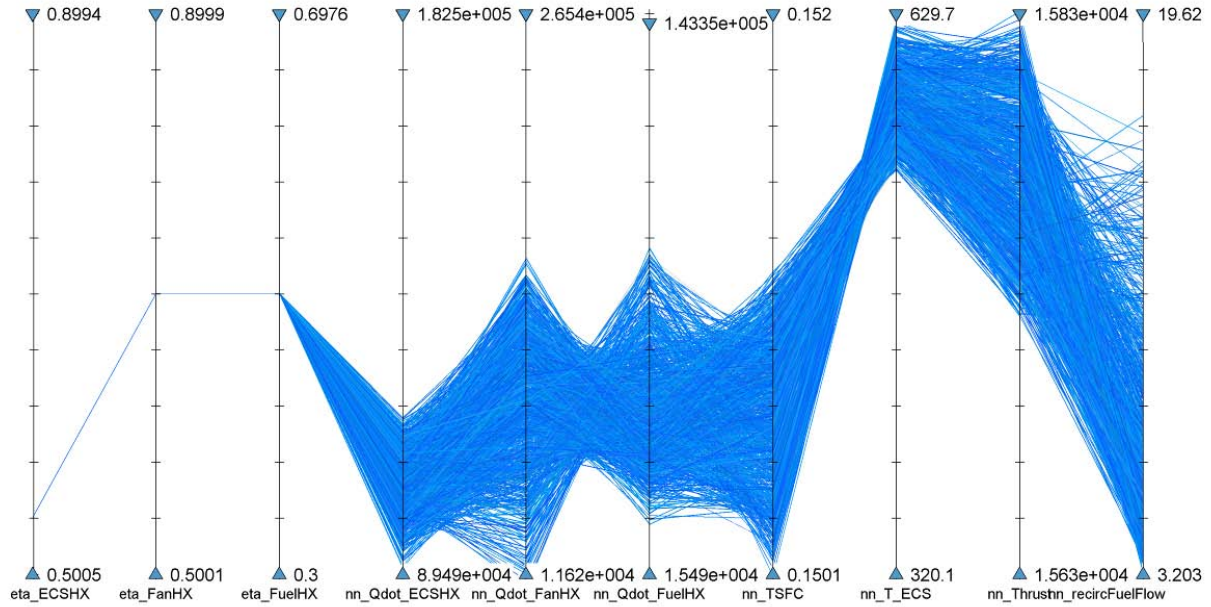

Figure 20: Reducing the effectiveness of the ECS heat exchanger has significant effects on all dependent variables except the recirculated fuel flow. (c.f. Figure 19. The only difference between Figure 19 and Figure 20 is the value of eta_ECSHX)

Conclusions

This report has presented the results of a project to demonstrate the effectiveness of multi-variate visualization methods for an aircraft energy system application. An aircraft thermal architecture including a fuel thermal management system, an air cycle machine for ECS cooling, and a turbofan engine were modeled in MATLAB. The model employs First-Law and Second-Law thermodynamic analyses to determine energy and transfers and entropy generation and is parameterized in terms of relevant system design variables including temperatures, heat exchanger properties, flow rates, and pressure ratios.

Using the MATLAB model, two parametric design space exploration studies were conducted for the baseline thermal system architecture using multi-variate data visualization and optimization approaches based on parallel coordinates. In the first study, heat transfer rates were specified directly, and in the second study, heat exchanger effectiveness was specified. The investigations focused on three primary aspects: (1) Identification of import design parameters driving system performance, (2) Second Law feasibility of heat transfers, and (3) optimality in terms of engine thrust and fuel burn performance. To conduct the studies, a design of experiments (DOE) was run using the MATLAB model. To allow rapid and interactive trade space explorations with parallel coordinates, artificial neural network surrogate models were regressed based on the DOE results.

The results of this small-scale seedling project have indicated significant utility of multi-variate visualization methods such as parallel coordinates for exploring the parametric design spaces of aircraft thermal systems to determine feasibility and optimality. Potential follow-on work could focus on investigations of alternate and/or improved studies including:

- Formal optimization algorithms to complement interactive design space filtering
- More complex thermal system architectures
- Mission simulations that capture air vehicle operational profiles and engine off-design performance and integrate fuel tank temperature
- Electrical system architectures
- Transient behavior

This initial project has necessarily been limited in scope, and the system that was modeled was a simple but representative example for demonstration purposes. Continued advancements in modeling, simulation, and design optimization capabilities will be required in order to keep pace with the advancing complexity of air vehicle system technologies and architectures.

References

[1]   Walters, E.A., Iden, S., McCarthy, K., Amrhein, M., O'Connell, T., Raczkowski, B., Wells, J., Lamm, P., Wolff, M., Yerkes, K., Borger, W., and Wampler, B., INVENT Modeling, Simulation, Analysis and Optimization, *48th AIAA Aerospace Sciences Meeting Including the New Horizons Forum and Aerospace Exposition,* January 4-7, 2010, Orlando, FL.

[2]   Bodie, M., Russell, G., McCarthy, K., Lucas, E., Zumberge, J., and Wolff, M., Thermal Analysis of an Integrated Aircraft Model, *48th AIAA Aerospace Sciences Meeting Including the New Horizons Forum and Aerospace Exposition,* January 4-7, 2010, Orlando, FL.

[3]   von Spakovsky, M. R., Riggins, D., and Marley, C., Non-Equilibirum Thermodynamic Issues Related to On-Demand Systems, *48th AIAA Aerospace Sciences Meeting Including the New Horizons Forum and Aerospace Exposition,* January 4-7, 2010, Orlando, FL.

[4]   Doty, J.H., Camberos, J. A., and Moorhouse, D. J., Benefits of Exergy-Based Analysis for Aerospace Engineering Applications: Part 1, *40th Thermophysics Conference,* June 23-26, 2008, Seattle, WA.

[5]   Doty, J.H., Camberos, J.A., and Moorhouse, D.J., Benefits of Exergy-Based Analysis for Aerospace Engineering Applications: Part 2, *47th AIAA Aerospace Sciences Meeting Including The New Horizons Forum and Aerospace Exposition,* January 5-8, 2009, Orlando, FL.

[6]   Figliola, R., Tipton, R., and Li, H., Exergy Approach to Decision-Based Design of Integrated Aircraft Thermal Systems, *Journal of Aircraft*, Vol.40, No.1, 2003, pp.49–55.

[7]   German, B.J., A Tank Heating Model for Aircraft Fuel Thermal Systems with Recirculation, *49th AIAA Aerospace Sciences Meeting including the New Horizons Forum and Aerospace Exposition,* 4 - 7 January 2011, Orlando, FL.

[8]   Çengel, Y.A., *Heat and Mass Transfer: A Practical Approach*, McGraw Hill, 2007.